

Wearable sensor network for lower limb angle estimation in robotics applications

Andres L. Jutinico^{1,2}, Gustavo A. R. Rodriguez², Julian Rolando Camargo Lopez¹

¹Department of Electronic Engineering, Faculty of Engineering, Universidad Distrital Francisco José de Caldas, Bogotá, Colombia

²Master of Information Sciences and Communications, Faculty of Engineering, Universidad Distrital Francisco José de Caldas, Bogotá, Colombia

Article Info

Article history:

Received Mar 02, 2022

Revised Sep 27, 2022

Accepted Oct 26, 2022

Keywords:

Angle estimation

IEEE 802.11 standard

Kalman filter

Wearable systems

Wireless sensor network

ABSTRACT

In human-robot interaction, sensors are relevant in guaranteeing stability and high performance in real-time applications. Nonetheless, accuracy and portable sensors for robots usually have high costs and little flexibility to process signals with free software. Therefore, we propose a wearable sensor network to measure lower limb angular position in human-robot interaction systems. The methodology employed to achieve the aim consisted in implementing a wireless network using low-cost devices, verifying design requirements, and making a validation via a proof of concept. The requirements to design the network include low loss of information, real-time communication, and sensor fusion to estimate the angular position using a gyroscope and accelerometer. Hence, the sensor network developed has a client-server architecture based on ESP8266 microcontrollers. In addition, this network uses the standard 802.11 b/g/n to transmit angular velocity and acceleration measures. Furthermore, we implement the user datagram protocol (UDP) protocol to operate in real-time with a sample time of 10 ms. Finally, we implement a proof of concept to show the system's effectiveness. Thus, we use the Kalman filter to estimate the angular position of the foot, shin, thigh, and hip. Results indicate that the implemented sensor network is suitable for real-time robotic applications.

This is an open access article under the [CC BY-SA](https://creativecommons.org/licenses/by-sa/4.0/) license.



Corresponding Author:

Andres L. Jutinico

Department of Electronic Engineering, Faculty of Engineering

Universidad Distrital Francisco José de Caldas, Bogotá, Colombia

Email: aljutinicoa@udistrital.edu.co

1. INTRODUCTION

Stroke is considered a frequent neurological emergency and constitutes the second leading cause of death globally, with 12.2 million cases per year and 6.55 million losses per year, respectively [1], [2]. In addition, this disease has become the leading cause of long-term disability affecting daily life activities. Moreover, this medical condition entails a socioeconomic impact with high costs in initial medical care and enormous difficulties for patients who usually need treatment and rehabilitation.

Research on robotics rehabilitation has put its efforts at the service of health. There are robots employed in human care, which are used to recover the activity of the locomotive systems of the human being. Examples of these technologies are exoskeletons and robotic platforms for rehabilitation [3]. In this sense, robots can support physical therapist work and help the user repeat training with a controlled and monitored intensity to promote neurogenesis and motor control [4]. Electronic instrumentation is an area to be applied in this type of robot, which is growing and contributes to diminishing the cost of the same, having a positive impact on society, and allowing for deeper studies or significant scientific contributions [5].

Commercially there are systems for acquiring kinematic and biomechanical signals used in robotic rehabilitation. However, these devices have high costs and little flexibility to process signals with free software. This article proposes a wearable sensor network to measure lower limb angular position in human-robot interaction systems. The network consists of three inertial measurement units (IMU) to determine limb acceleration and angular velocity. The angular position is estimated and processed by ESP8266 microcontrollers. Furthermore, this sensor network uses the 802.11b/g/n standard for interconnection with a host by the user datagram protocol (UDP). Finally, we validate the system operation by a proof of concept, estimating the angular position through the Kalman filter.

Industrial communications are used to supervise physical, chemical, and environmental variables, among others. In this kind of system, wired networks guarantee the integrity of the data. Therefore, nodes can work in a distributed way and using specific protocols, such as standard wired communication protocols: RS-485, highway addressable remote transducer (HART), Profibus, Ethernet, and Modbus. In robotic applications, the selection of communication systems is also given by guaranteeing data integrity. Nevertheless, the device's portability plays an essential role in adjusting sensor networks with mechatronic devices. Currently, communication systems use several protocols for transferring information over wireless means with different bandwidths and frequencies of operation, highlighting communication protocols such as Bluetooth, Zigbee, and WiFi, among others [6], [7].

Wireless sensor networks include a set of devices to measure variables of a process and transmit them over small or long distances [8], [9]. Sensor networks are regularly provided with a server or a base station that serves as a reference point for receiving information, operating in most cases with homogeneous devices according to the nodal distribution. These nodes generally can process and store information and have various sensors. However, they do not necessarily have to be the same. Conventionally, nodes have sensors, controllers, communication modules, and microprocessors. Depending on the purpose of development, the processing applications will have varying levels of complexity, either to capture the information or to analyze it [10].

Around the world, there are prototypes and commercial systems that focus on motor rehabilitation using robotics. These robots use a wide variety of communication protocols for sensors. Biofeedback systems are widely used in patients with balance disorders due to vestibular loss, stroke, or aging. In addition, patients often undergo continuous balance training regimens with the help of biofeedback systems that can effectively increase postural stability. For example, Alahakone and Senanayake [11] employ a wireless inertial sensor for trunk tilt angle measurements, a complete software with an interface for data acquisition, processing, and visualization. The system allows video recording, feedback signal generation, data analysis, and portable vibrating actuators to provide feedback. In [12] developed the inertia-based detection modality with increased biofeedback to study trunk swing and a training protocol for clinical evaluation. In [13] show a wireless insole sensor biofeedback and gait analysis system to rehabilitate balance control for post-stroke patients. The system integrates a wireless network of home and open-source electronic healthcare sensors to be used with mobile devices. In [14] highlight ZigBee's higher communication efficiency and lower power consumption. In addition, they show a comparison between ZigBee and Bluetooth serial port profiles for wireless body-area sensor networks. The system called Kimera is a portable brain-computer interface (BCI) with wireless information transfer mechanisms that consists of two layers of hardware architecture, data acquisition, and wireless transmission by a Bluetooth ARM chip [15]. In [16] present a wearable multi-sensor system for human motion monitoring for use in rehabilitation. This system integrates five small wireless modules, interconnected with accelerometer data at high frequency, synchronized by an external master device, making the system ideal for patient monitoring. Wireless biomedical implants are the subject of research in wireless body area networks (WBAN). For example, the incremental relaying communication protocol based on mutual information (MI) is presented [8]. The communication path selection is given by the deeply implanted and the receiver distance. The results show that the MI-based incremental retransmission technique achieves better performance compared to other proposed techniques. In [17] show a study to validate the accuracy of the inertial measurement unit-based knee angle measurement system during physiotherapy exercises. The used system has a mobile application for recording these data.

Robots for rehabilitation must measure biosignals to promote motor control and safe in human-robot interaction. In this context, sensors must couple on the robot and the human and transfer data by a network. There are several examples of this: the robotic training system for upper limb rehabilitation counts with an exoskeleton that allows the therapist to modify the patient's routine. The robot supports various trajectories and repetitions followed by the exoskeleton in the shoulder, elbow, and wrist joints. The robot has sensors for angular position and electromyographic (EMG) signals and a user interface developed in LabView [18]. NOTTABIKE is a robot designed to investigate and promote lower limb motor control by using a platform that owns a bike for exercise. This device has a servo motor, angular encoders, pedals, force-torque sensors, and an EMG system [19]. In [20] shows the design and control of an active knee orthosis driven by a rotary series elastic actuator (SEA).

The custom rotary SEA is responsible for driving an active knee orthosis and allowing the torque measurement. Then, the user attaches the robot to its body and executes controlled movements [21]. The system robotic platform for ankle rehabilitation uses a SEA for control and force measurement, a sensor for the angular position, and EMG. In [4], [22] introduce a Markovian force and impedance control for human-robot interaction in this type of robot. The exoskeleton reported in [23] is a mechatronic device to assist in passive physiotherapy. The robot follows computer-generated trajectories of knee and ankle joints. Peña *et al.* [20] propose an EMG-driven adaptive impedance control to improve user engagement during the rehabilitation session by considering an active knee orthosis. Another example of EMG sensing where Sartori *et al.* [24] used EMG data to build a musculoskeletal model to predict stiffness in the human ankle and knee joints.

The contribution of the estimation of angular positions in robotic rehabilitation improves the performance and efficiency of therapies. Some research has used the Kalman filter for this aim. In [25] is shown a standard angular estimation approach by Kalman filters for lower limb exoskeletons for inertial measurement unit (IMU) based on individual link configurations. In [26], introduce a global approach to estimate absolute angles of the lower limb segments by the Kalman filter. This approach uses inertial sensors and the exoskeleton encoder facilitating gait analysis and exoskeleton control.

2. METHOD

2.1. Communication topology

Figure 1 shows the overall configuration of the proposed network sensors. The system uses three nodes, each with the inertial measurement unit (IMU) sensor and a microcontroller with a communication wifi module. The sensors are located at the foot, shin, femur, and hip height and transmit sensors data to a server implemented in a microcontroller. The communication system uses the UDP protocol to transfer the information to a computer that stores the data in files for collection and processing.

UDP protocol is in the transport layer of the open systems interconnection model (OSI model) and can be used according to standard 802.11. The protocol provides a datagram exchange service over the network; therefore, it cannot ensure the delivery of datagrams or packets. In this project, the UDP protocol was selected since it is not possible to carry out measurement retransmissions due to the strict delay requirements of the system. Each node (is to say, the clients) counts with an inertial measurement unit MPU6050 and an ESP8266 microcontroller, which has an 802.11 communication module. Besides, the server uses an ESP8266 microcontroller to establish wireless communication and send the data to the computer by a USB wire. Notice that the information sent from sensors in UDP datagrams does not establish a two-way connection to the server since we are looking for real-time one-way and not the arrival confirmation. Figure 2 shows the workflow to save data from the sensors. First, devices are started. The following is to establish the connection between nodes and the server. Then to accomplish this requirement, there is a timeout condition for server response until 30 s. Once establish this connection each sensor is linked and begins data detection, and data values are saved.

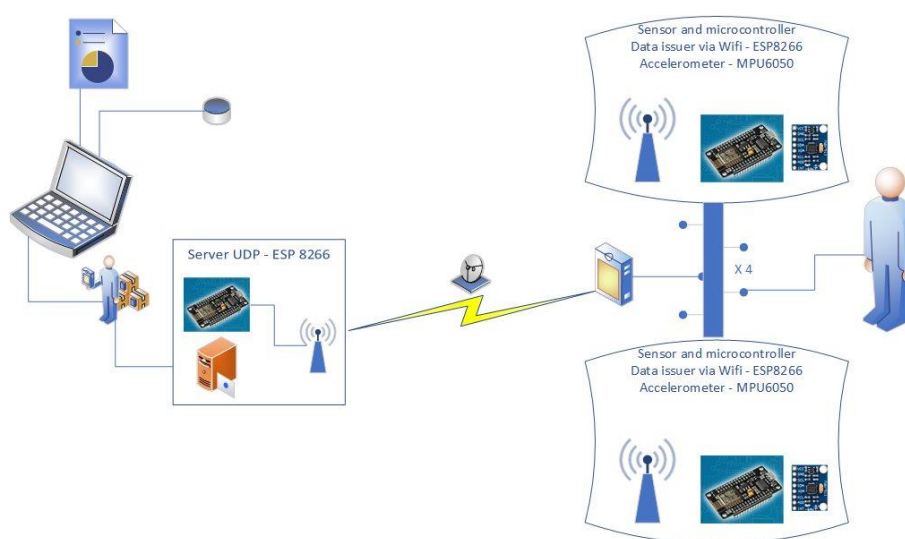


Figure 1. The overall configuration of the proposed network sensors

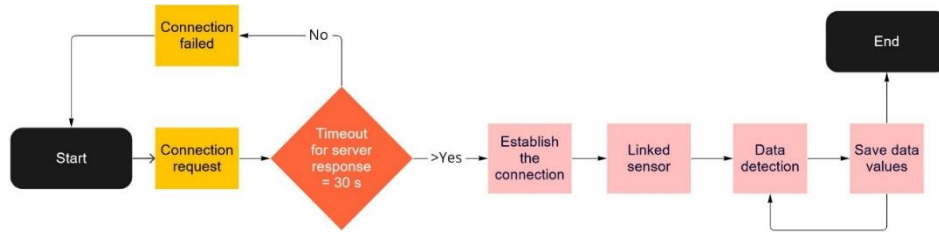


Figure 2. Workflow to save data from the sensors

2.2. Mathematical model of acceleration and angular velocity

IMU are attached to each segment of the body as shown in Figure 3. The angular velocity in each limb is modeled as:

$$\dot{\theta}(t) = \dot{\theta}_g(t) + b_g(t) + \eta_g(t) \quad (1)$$

$$\dot{b}(t) = -\frac{1}{\tau_g} b_g(t) + \eta_{bg}(t) \quad (2)$$

Where $\dot{\theta}_g(t)$ is the measurement angular velocity from the gyroscope, $\eta_g(t)$ is the Gaussian noise with variance σ_g^2 , $b_g(t)$ representing the bias of the gyroscope, τ_g is the Markov process correlation time and η_{bg} is the white Gaussian noise with variance σ_{bg}^2 .

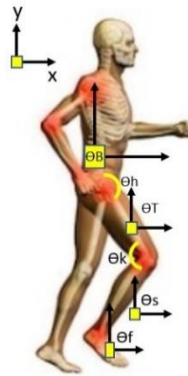


Figure 3. Location of IMU

The acceleration of each link, $a(t)$, in an instant of time, t , is modeled as:

$$a(t) = a_a(t) + b_a(t) + \mu_a(t) \quad (3)$$

$$\dot{b}_a(t) = -\frac{1}{\tau_a} b_a(t) + \mu_{ba}(t) \quad (4)$$

Where $a_a(t)$ is the acceleration obtained from the accelerometer on the x -axis of the local coordinate system, $\mu_a(t)$ is the Gaussian noise with variance σ_a^2 , $b_a(t)$ is the bias of the accelerometer, τ_a is the Markov process correlation time and $\mu_{ba}(t)$ is white Gaussian noise with variance σ_{ba}^2 .

2.3. Strategy for sensor fusion

In this section, the angular position estimation of each link is obtained from sensor fusion, using measures of acceleration and angular velocity. In this paper, the selected method to make sensor fusion is the Kalman filter. This filter uses the gyroscope signal as the primary source for position estimation. The accelerometer signal is considered redundant information to correct the estimated value of the gyroscope that is affected by integration errors. The angular velocity estimated by the gyroscope and the bias are modeled as:

$$\hat{\theta}_g(t) = \dot{\theta}_g(t) + \hat{b}_g(t) \quad (5)$$

$$\dot{\hat{b}}_g(t) = -\frac{1}{\tau_g} \hat{b}_g(t) \quad (6)$$

Therefore, the difference between actual and estimated values is:

$$\begin{aligned} \Delta\hat{\theta}(t) &= \hat{\theta}(t) - \hat{\hat{\theta}}(t) \\ &= b_g(t) - \hat{b}_g(t) + \eta_{bg}(t) \\ &= \Delta b_g(t) + \eta_{bg}(t) \end{aligned} \quad (7)$$

And,

$$\begin{aligned} \Delta\dot{b}_g(t) &= \dot{b}_g(t) - \dot{\hat{b}}_g(t) \\ &= -\frac{1}{\tau_g} (b_g(t) - \hat{b}_g(t)) + \eta_{bg}(t) \\ &= -\frac{1}{\tau_g} \Delta b_g(t) + \eta_{bg}(t) \end{aligned} \quad (8)$$

Thus, the state space representation of the estimation system is given by:

$$\begin{bmatrix} \Delta\dot{\theta}(t) \\ \Delta\dot{b}_g(t) \end{bmatrix} = \begin{bmatrix} 0 & 1 \\ 0 & -\frac{1}{\tau_g} \end{bmatrix} \begin{bmatrix} \Delta\theta(t) \\ \Delta b_g(t) \end{bmatrix} + \begin{bmatrix} 1 & 0 \\ 0 & 1 \end{bmatrix} \begin{bmatrix} \eta_{g}(t) \\ \eta_b(t) \end{bmatrix} \quad (9)$$

$$\dot{x} = Ax(t) + B\omega(t) \quad (10)$$

Where $\Delta\theta(t)$ and $\Delta b_g(t)$ are the position estimation and offset errors of the gyroscope, respectively. The states of the systems are x , ω is the white Gaussian noise, and A and B are parametric matrices that represent the model (9). The angular position obtained from the accelerometer is given by:

$$\hat{\theta}_a(t) = \arcsin\left(\frac{a_a}{g_e}\right) = \theta(t) + \eta_a(t) \quad (11)$$

Where g_e is the gravitational acceleration value on the x axis. Notice that no is considered dynamic accelerations. The output equation of the state space representation is given by the difference between the estimated position of the accelerometer and the estimated position of the gyroscope.

$$\begin{aligned} z(t) &= \hat{\theta}_a(t) - \hat{\theta}_g(t), \\ &= \theta(t) + \eta_a(t) - \hat{\theta}_g(t) \\ &= \Delta\theta(t) + \eta_a(t). \end{aligned} \quad (12)$$

Thus, the estimated values for the angular position and gyroscope error are given by:

$$z = Cx(t) + v(t) = [1 \quad 0] \begin{bmatrix} \Delta\theta(t) \\ \Delta b_g(t) \end{bmatrix} + \eta_a(t) \quad (13)$$

$$\hat{\theta}(t) = \hat{\theta}_g(t) + \Delta\hat{\theta}(t) \quad (14)$$

$$\hat{b}(t) = \hat{b}_g(t) + \Delta\hat{b}_g(t) \quad (15)$$

Where C is a parametric matrix, v represent a random error, and $\Delta\hat{\theta}(t)$ and $\Delta\hat{b}_g(t)$ are estimated angular position values and compensation errors, respectively.

3. RESULTS AND DISCUSSION

To validate the developed system, we made a test where a user walked for a straight line of 10 meters. The test had an approximate duration of 12 seconds. The trial started once the communication system was linked by wifi to the UDP server. Sensors were located at the foot, shin, femur, and hip height, as is shown in Figure 4(a) and Figure 4(b) shows the electronic device for each node.

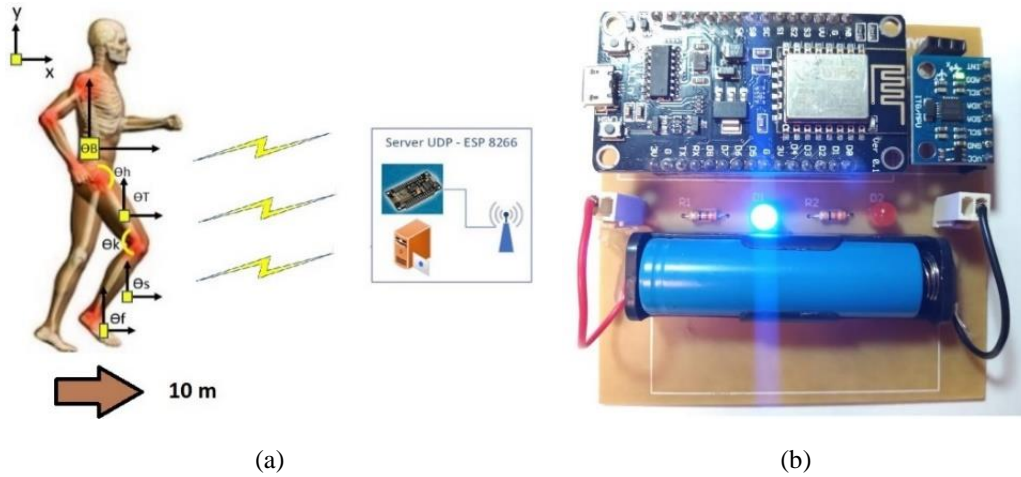


Figure 4. Test for system validation: (a) ten meter test and (b) node

3.1. Angular position estimation using Kalman filter

To validate the system, we perform a proof of concept. For this proof, a healthy user walked for ten meters while the sensors network transmitted each limb's acceleration and angular velocity. Furthermore, we compared the estimation results from the Kalman filter with the estimation given by a complementary filter. For the calculation of the angular position from the speed measurement performed by the gyroscope, it is necessary to consider the resolution of the sensor. Therefore, the following conversion factor is used:

$$G_R = \frac{2^n}{250^\circ/s} \quad (16)$$

Where $n = 16$ is the number of bits used by the sensor, and 250 is a parameter taken from the sensor datasheet. Therefore, $\omega(k) = \bar{\omega}(k)/G_R$, where $\bar{\omega}$ is the gyroscope measure. The angular position can be performed from the following integrative recursion.

$$\theta_{xg}(k) = \tau_s \omega(k-1) + \theta_{xg}(k-1) \quad (17)$$

We use a sample time $T_s = 10$ ms. Figure 5 shows the $\theta_{xg}(k)$ angle estimation for the foot sensor during the experiment. We highlight that the velocity integration of the gyroscope causes an angular bias. For the calculation of the angular position from the measurement of the acceleration performed by the sensor, the resolution of the sensor should be considered, therefore the following conversion factor is used:

$$A_R = \frac{2^n}{4 \times 9.81 \text{ m/s}^2} \quad (18)$$

Where $n = 16$ is the number of bits used by the IMU, and $g = 9.81 \text{ m/s}^2$ is the gravity. Thus, $a_x(k) = \bar{a}_x(k)/A_R$, where \bar{a}_x is the accelerometer measure. The angular position relative to the x -axis can be estimated according with (11), as:

$$\theta_{xa} = \arcsin(a_x/g) \quad (19)$$

Figure 5 shows the result of estimating the angle from accelerometer signal θ_{xa} . From the bottom figure, it is appreciated that, although the signal has no bias, it is characterized by a large amount of noise. This graph shows the need for sensory fusion to perform a more accurate angular position calculation.

The angular estimation by the Kalman filter consider the model described in (9) and (13), where $\Delta\theta(t) = \hat{\theta}_a(t) - \hat{\theta}_g(t)$, is the difference between the angle calculated from the accelerometer and the angle calculated from the gyroscope. The noise produced in the acceleration measurement is modeled by $\eta_a(t)$. The Q_n and R_n are weighting matrices that represent the noise covariance in the states and output signal of the model according to:

$$Q_n = \begin{bmatrix} \sigma_g^2 & 0 \\ 0 & \sigma_{bg}^2 \end{bmatrix}, \quad R_n = \sigma_a^2 \quad (20)$$

The parameters of the model in (9), (13), and (20) are shown in Table 1. The angular position estimation for each sensor is performed according to Kalman’s classic filter equation:

$$\hat{x}(k + 1) = F\hat{x}(k) + L(\Delta\theta(k) - C\hat{x}(k)) \tag{21}$$

Where $\hat{x}(k) = [\Delta\hat{\theta}(k) \Delta\hat{b}_g(k)]'$ are the states estimated by the Kalman filter, F is the equivalent of matrix A for the discrete-time with the sample-time T_s , k is the discrete-time iteration and L is de Kalman vector.

Finally, the estimate of the angular position using sensory fusion is calculated in (22) and Table 2. shows the Kalman vector for each link.

$$\hat{\theta}(k) = \theta_{xg}(k) + \Delta\hat{\theta}(k|k) \tag{22}$$

Figure 6 shows the result of the proof of concept developed to validate the sensor network. Each figure at the top shows signals for $\Delta\theta$ (blue) and $\Delta\hat{\theta}$ (red) used to estimate the angle of the respective link. At the bottom, each figure shows the estimation by the Kalman filter (KF in blue color) compared to a standard complementary filter (CF in red color). Angular position estimations for foot, shin, thigh, and hip are shown in Figure 6(a) to Figure 6(d) respectively. In this experiment, results indicate that for ten-meter walking test is clear that the two estimates are similar. However, the estimates obtained with KF result in lower amplitude peaks.

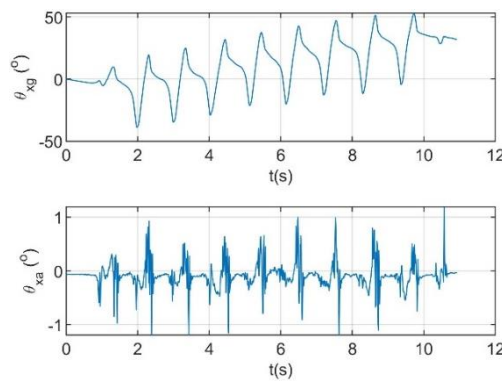


Figure 5. Estimation of the foot angular position by gyroscope and accelerometer signals

Figure 6(a) shows the result of estimating the angle of the foot. The sensor was placed on the user’s shoe so that the starting angle is -18.8° relative to the x coordinate axis. The maximum and minimum angular position values obtained with the Kalman filter were 8.62° and -52.36° , respectively. The maximum and minimum angular position values obtained with the complementary filter were 16.76° and -61.48° , respectively. Figure 6(b) shows the result of estimating the angle of the shin. The starting angle is 80.5° relative to the x coordinate axis. The maximum and minimum angular position values obtained with the Kalman filter were 103.96° and 25.8° , respectively.

The maximum and minimum angular position values obtained with the complementary filter were 16.76° and -61.48° , respectively. Figure 6(c) shows the result of estimating the angle of the thigh. The starting angle is 67.5° relative to the x coordinate axis. The maximum and minimum angular position values obtained with the Kalman filter were 80.4° and 45.59° , respectively. The maximum and minimum angular position values obtained with the complementary filter were 82.66° and 38.51° , respectively. Figure 6(d) shows the result of estimating the angle of the hip. The starting angle is 59.22° relative to the x coordinate axis. The maximum and minimum angular position values obtained with the Kalman filter were 65.73° and 49.14° , respectively. The maximum and minimum angular position values obtained with the complementary filter were 67.51° and 46.82° , respectively.

Table 1. Parameters for Kalman filter calculation for each inertial sensor

Kalman filter	σ_g	σ_{b_g}	σ_a	τ_g
Hip	0.0103	30	46.56	839.7
Thigh	0.0017	50	329.08	2138.5
Shin	0.0008	96.4	100.94	1465.3
Foot	291.2	18.594	291.29	3567.5

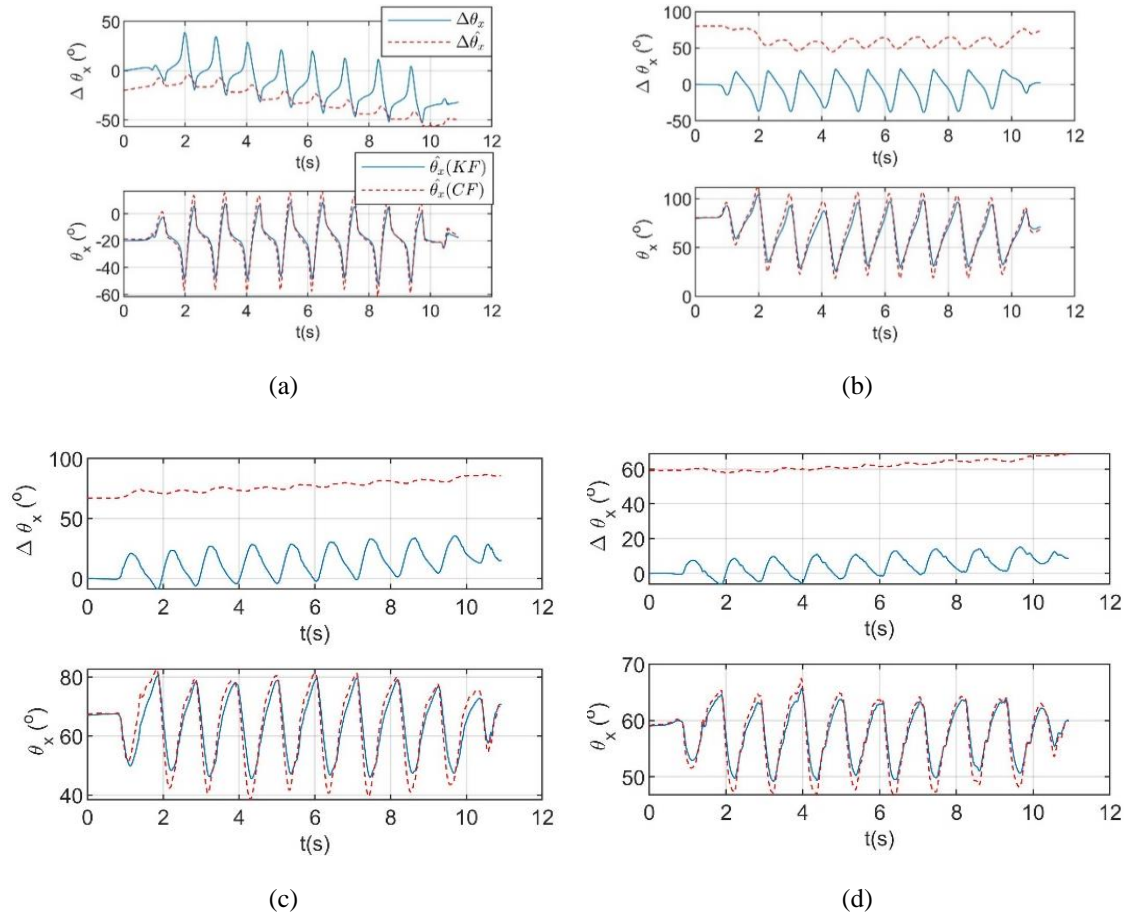


Figure 6. Results of estimating angular position for: (a) foot, (b) shin, (c) thigh, and (d) hip

Table 2. Kalman vector for each link

Kalman filter	Kalman's constant: L
Hip	$\begin{bmatrix} 0.0137 \\ 0.0006 \end{bmatrix}$
Thigh	$\begin{bmatrix} 0.0055 \\ 0.0015 \end{bmatrix}$
Shin	$\begin{bmatrix} 0.0138 \\ 0.0095 \end{bmatrix}$
Foot	$\begin{bmatrix} 0.0113 \\ 0.0064 \end{bmatrix}$

4. CONCLUSION

This article shows a sensor network for angle estimation of lower limbs. We highlight that this network configuration is proper for robotic rehabilitation environments since devices are wearables and wireless. This network has an ESP8266 microcontroller for processing and communication in each node. The communication between nodes and the server is carried out by the standard 802.11 b/g/n. We use the client-server architecture with UDP protocol which allows a sample time of 10 ms. The Wi-Fi use allows an intuitive connection and stable communication between nodes and the server. We performed a proof of concept to validate the implemented sensor network and used the Kalman filter to estimate the angular position of the foot, shin, thigh, and hip. The Kalman filter allowed sensor fusion from angular velocity and acceleration measurements by the MPU6050 in each node. In this sense, the Kalman filter estimates the angle error due to the numerical integration of angular velocity given by the gyroscope. Also, it diminishes the noise from the angular position coming from the accelerometer. Therefore, we compensate the actual measurement to obtain an accuracy angle. Results show that this sensor network is suitable for real-time robotic applications. In future works, we hope to use this sensor network to combine kinematic and electromyographic signals in applications for rehabilitation.

ACKNOWLEDGEMENTS

The authors are grateful to the Universidad Distrital Francisco José de Caldas. This work is supported by Universidad Distrital Francisco José de Caldas under project 2-5-617-20.

REFERENCES

- [1] V. L. Feigin *et al.*, “Global, regional, and national burden of stroke and its risk factors, 1990–2019: a systematic analysis for the Global Burden of Disease Study 2019,” *The Lancet Neurology*, vol. 20, no. 10, pp. 795–820, 2021, doi: 10.1016/S1474-4422(21)00252-0.
- [2] V. L. Feigin *et al.*, “World Stroke Organization (WSO): Global Stroke Fact Sheet 2022,” *International Journal of Stroke*, vol. 17, no. 1, 2022, doi: 10.1177/17474930211065917.
- [3] D. S. -Méndez, M. A. -Montiel, and E. L. -González, “Design of an Exoskeleton Prototype for Shoulder Rehabilitation,” *Revista Mexicana de Ingeniería Biomedica*, vol. 38, no. 1, pp. 330–342, 2017. [Online]. Available: <https://www.scielo.org.mx/pdf/rmib/v38n1/2395-9126-rmib-38-01-330.pdf>
- [4] F. M. Escalante, A. L. Jutinico, J. C. Jaimes, M. H. Terra, and A. A. G. Siqueira, “Markovian Robust Filtering and Control Applied to Rehabilitation Robotics,” *IEEE/ASME Transactions on Mechatronics*, vol. 26, no. 1, pp. 491–502, 2021, doi: 10.1109/TMECH.2020.3034245.
- [5] K. Nizamis, A. Athanasiou, S. Almpani, C. Dimitrousis, and A. Astaras, “Converging Robotic Technologies in Targeted Neural Rehabilitation: A Review of Emerging Solutions and Challenges,” *Sensors*, vol. 21, no. 6, 2021, doi: 10.3390/s21062084.
- [6] C. A. V. -Romero, J. E. B. -Jaimes, and D. C. P. -González, “Configuration Parameters in Module XBEE-PRO® ZB S2B for Measuring Environmental Variables,” *Tecnura*, vol. 19, no. 45, pp. 141–157, 2015, doi: 10.14483/udistrital.jour.tecnura.2015.3.a011.
- [7] C. Cifuentes, A. Braidot, L. Rodríguez, M. Frisoli, A. Santiago, and A. Frizzera, “Development of a wearable ZigBee sensor system for upper limb rehabilitation robotics,” in *2012 4th IEEE RAS + EMBS International Conference on Biomedical Robotics and Biomechatronics (BioRob)*, 2012, pp. 1989–1994, doi: 10.1109/BioRob.2012.6290926.
- [8] Y. Liao, M. S. Leeson, Q. Cai, Q. Ai, and Q. Liu, “Mutual-information-based incremental relaying communications for wireless biomedical implant systems,” *Sensors*, vol. 18, no. 2, 2018, doi: 10.3390/s18020515.
- [9] D. Goyal and Sonal, “Power management in Wireless Sensor Network,” in *2016 3rd International Conference on Computing for Sustainable Global Development (INDIACom)*, 2016, pp. 598–601. [Online]. Available: <https://ieeexplore.ieee.org/document/7724333>
- [10] K. Sohrawy, D. Minoli, and T. Znati, *Wireless sensor networks: Technology, Protocols, and Applications*, Hoboken, NJ, USA: Wiley Telecom, John Wiley & Sons, Inc., 2007. [Online]. Available: <https://www.wiley.com/en-us/Wireless+Sensor+Networks%3A+Technology%2C+Protocols%2C+and+Applications-p-9780470112755>
- [11] A. U. Alahakone and S. M. N. A. Senanayake, “A combination of inertial sensors and vibrotactile feedback for balance improvements in therapeutic applications,” in *Proc. 2009 Innovative Technologies in Intelligent Systems and Industrial Applications, CITISIA 2009*, 2009, pp. 5–10, doi: 10.1109/CITISIA.2009.5224252.
- [12] A. Kos and A. Umek, “Reliable Communication Protocol for Coach Based Augmented Biofeedback Applications in Swimming,” *Procedia Computer Science*, vol. 174, pp. 351–357, 2020, doi: 10.1016/j.procs.2020.06.098.
- [13] A. Johansson, W. Shen, and Y. Xu, “An ANT based wireless body sensor biofeedback network for medical E-health care,” in *Proc. 7th International Conference on Wireless Communications, Networking and Mobile Computing*, 2011, pp. 1–5, doi: 10.1109/wicom.2011.6040656.
- [14] M. Benocci, E. Farella, L. Benini and L. Vanzago, “Optimizing ZigBee for data streaming in body-area bio-feedback applications,” *2009 3rd International Workshop on Advances in sensors and Interfaces*, 2009, pp. 150–155, doi: 10.1109/IWASI.2009.5184786.
- [15] L. Maggi, S. Parini, L. Piccini, G. Panfili, and G. Andreoni, “A four command BCI system based on the SSVEP protocol,” in *2006 International Conference of the IEEE Engineering in Medicine and Biology Society*, 2006, pp. 1264–1267, doi: 10.1109/IEMBS.2006.260353.
- [16] L. G. -Villanueva, S. Cagnoni, and L. Ascari, “Design of a wearable sensing system for human motion monitoring in physical rehabilitation,” *Sensors*, vol. 13, no. 6, pp. 7735–7755, 2013, doi: 10.3390/s130607735.
- [17] K. M. Bell *et al.*, “Verification of a portable motion tracking system for remote management of physical rehabilitation of the knee,” *Sensors*, vol. 19, no. 5, 2019, doi: 10.3390/s19051021.
- [18] M. T. -Quezada, R. S. -Zamora, L. B. -Vázquez, D. D. -Rodríguez, and A. L. -Delis, “Robotic training system for upper limb rehabilitation,” *Ingeniería y Universidad*, vol. 18, no. 2, pp. 235–252, 2014, doi: 10.11144/Javeriana.IYU18-2.rtsu.
- [19] A. R. D. -Elli and P. G. Adamczyk, “Design and Validation of a Lower-Limb Haptic Rehabilitation Robot,” *IEEE Transactions on Neural Systems and Rehabilitation Engineering*, vol. 28, no. 7, pp. 1584–1594, 2020, doi: 10.1109/TNSRE.2020.3000735.
- [20] G. G. Peña, L. J. Consoni, W. M. dos Santos, and A. A. G. Siqueira, “Feasibility of an optimal EMG-driven adaptive impedance control applied to an active knee orthosis,” *Robotics and Autonomous Systems*, vol. 112, pp. 98–108, 2019, doi: 10.1016/j.robot.2018.11.011.
- [21] F. M. Escalante, J. C. P. -Ibarra, J. C. Jaimes, A. A. G. Siqueira, and M. H. Terra, “Robust Markovian Impedance Control applied to a modular knee-exoskeleton applied to a modular knee-exoskeleton,” *IFAC-PapersOnLine*, vol. 53, no. 2, pp. 10141–10147, 2020, doi: 10.1016/j.ifacol.2020.12.2740.
- [22] A. L. Jutinico, O. F. -Cediel, and A. A. G. Siqueira, “Complementary stability of Markovian systems: Series elastic actuators and human-robot interaction,” *IFAC-PapersOnLine*, vol. 54, no. 4, pp. 112–117, 2021, doi: 10.1016/j.ifacol.2021.10.019.
- [23] R. L. -Gutiérrez, H. A. -Sierra, S. Salazar, and R. Lozano, “Adaptive control in passive rehabilitation routines using ELLTIO,” *Revista Mexicana de Ingeniería Biomedica*, vol. 38, no. 2, pp. 458–478, 2017, doi: 10.17488/RMIB.38.2.3.
- [24] M. Sartori, M. Maculan, C. Pizzolato, M. Reggiani, and D. Farina, “Modeling and simulating the neuromuscular mechanisms regulating ankle and knee joint stiffness during human locomotion,” *Journal of Neurophysiology*, vol. 114, no. 4, pp. 2509–2527, 2015, doi: 10.1152/jn.00989.2014.
- [25] S. L. Nogueira, A. A. G. Siqueira, R. S. Inoue, and M. H. Terra, “Markov Jump Linear Systems-based position estimation for lower limb exoskeletons,” *Sensors*, vol. 14, no. 1, pp. 1835–1849, 2014, doi: 10.3390/s140101835.
- [26] S. L. Nogueira *et al.*, “Global Kalman filter approaches to estimate absolute angles of lower limb segments,” *BioMedical Engineering Online*, vol. 16, no. 58, 2017, doi: 10.1186/s12938-017-0346-7.

BIOGRAPHIES OF AUTHORS

Andres L. Jutinico    received the bachelor's in electronic engineering from The Universidad Distrital Francisco José de Caldas, Bogota, Colombia, in 2005, the M.Sc. degree in industrial automation from the National University of Colombia, in 2012, and the Ph.D. degree in mechanical engineering from the University of São Paulo, Brazil, in 2019. His current research interests include control systems, assistive and rehabilitation robotics, and sensor fusion for assistive technology. He can be contacted at email: aljutinicoa@udistrital.edu.co.



Gustavo A. R. Rodríguez    received the bachelor's in electronic engineering from The Universidad Distrital Francisco José de Caldas, Bogota, Colombia, in 2015, the M.Sc. information and communication sciences with an emphasis on teleinformatics in 2022. His current research interests include control systems, assistive and rehabilitation robotics, and sensor fusion for assistive technology. He can be contacted at email: garodriguezr@correo.udistrital.edu.co.



Julian Rolando Camargo Lopez    is an Associate Professor of Faculty of Engineering at Universidad Distrital Francisco José de Caldas in Bogotá, Colombia. Electronic Engineer from the Universidad Distrital Francisco José de Caldas, Specialist in Design and Construction of Telematic Solutions from the Autonomía University of Colombia, master's in information and communications sciences from Universidad Distrital Francisco José de Caldas. He can be contacted at email: jcamargo@udistrital.edu.co.